

The Influence of Corneoscleral Topography on Soft Contact Lens Fit

Lee A. Hall,^{1,2} Graeme Young,¹ James S. Wolffsohn,² and Colleen Riley³

PURPOSE. To evaluate the influence of peripheral ocular topography, as evaluated by optical coherence tomography (OCT), compared with traditional measures of corneal profile using keratometry and videokeratoscopy, on soft contact lens fit.

METHODS. Ocular surface topography was analyzed in 50 subjects aged 22.8 years (SD ± 5.0) using videokeratoscopy (central keratometry, corneal height, and shape factor) and OCT to give both full sagittal cross-sections of the cornea and cross-sections of the corneoscleral junctions. Corneoscleral junction angle, corneal diameter, corneal sagittal height, and scleral radius were analyzed from the images. Horizontal visible iris diameter and vertical palpebral aperture were analyzed from digital slit lamp images. Lens fit was graded after 30 minutes wear of a -2.50 D commercially available standard hydrogel (etafilcon A, modulus 0.30 MPa) and silicone hydrogel (galyfilcon A, 0.43 MPa) design of similar geometries (8.30-mm base curve, 14.0-mm diameter).

RESULTS. The mean horizontal corneal diameter was 13.39 mm (SD ± 0.44). In many cases, there was a tangential transition at the corneoscleral junction. The corneoscleral shape profile analyzed from cross-sectional OCT images contributed significantly ($P < 0.001$) to the prediction of soft contact lens fit compared with keratometry and videokeratoscopy, accounting for up to 24% of the variance in lens movement. The fit of the stiffer material silicone hydrogel lens was better able to be predicted and was more varied than the hydrogel contact lens.

CONCLUSIONS. The extra peripheral corneoscleral data gained from OCT characterization of ocular surface architecture provide valuable insight into soft contact lens fit dynamics. (*Invest Ophthalmol Vis Sci.* 2011;52:6801–6806) DOI:10.1167/iovs.11-7177

Suboptimal soft contact lens fit has been associated with discomfort,¹ poor vision,¹ physiological changes,^{2,3} and drop out from wear.⁴ Accurate predictors of soft lens fit to explain why lens fit varies between eyes would therefore be desirable aids to the fitting process. The selection of the initial base curve has traditionally been based on central corneal curvature, as measured by keratometry. The underlying assumption behind this is that steeper corneas have greater sagittal height and, therefore, require a lens of greater sagittal

depth in the form of a steeper base curve to optimally fit the cornea.⁵ Ocular sagittal height, though, is governed not just by central corneal curvature but also by corneal diameter, corneal shape factor, and the peripheral corneoscleral profile.^{6,7} Most soft contact lens diameters range from 13.8 to 14.2 mm and, hence, drape over the limbus onto the sclera by approximately 1 mm all around. Consequently, keratometry can be considered an oversimplified predictor of soft lens fit, and previous studies have shown that there is no strong correlation between keratometry readings and the best-fitting soft contact lens.^{7,8}

Computerized videokeratoscopy allows a more complete characterization of the corneal topography, with modern topographers capturing many thousands of data points across the corneal surface compared to that of only four in conventional keratometry. Their usefulness in the fitting of rigid contact lenses has been well documented.^{9,10} However, comparatively little work has been published regarding their application in soft lens fitting, and a recent study of soft lens fit showed only weak correlations.⁷

Although videokeratoscopy measurements have facilitated the collection of accurate data relating to the central and midperipheral cornea, information on the topography of the peripheral cornea, corneoscleral junction, and limbal sclera is scarce.^{11,12} It seems likely, however, that this area has the most influence on soft lens fit since this is where lenses are required to make the greatest flexural changes in order to align to the ocular surface.¹³

Ocular coherence tomography (OCT) has allowed for more extensive and detailed imaging of the anterior segment and peripheral corneoscleral profile. The imaging of soft contact lenses using OCT was first reported by Kaluzny and colleagues in 2002¹⁴ and then more recently¹⁵ using high-resolution spectral OCT. Shen and colleagues¹⁶ described the use of a custom-built OCT device to image an entire contact lens both in vivo and in vitro.

The purpose of this study was to evaluate the predictive value of peripheral ocular topography, as evaluated with OCT, on soft contact lens fit compared with traditional measures of corneal profile using keratometry and videokeratoscopy. It was expected that the corneoscleral shape profile would have a greater influence on lens fit than that predicted by corneal shape alone, partially explaining why lens fit varies between eyes with similar keratometry values. In addition, that lens fit would demonstrate a wider range with a stiffer contact lens material, in turn, contributing to the differences in lens fit seen clinically between soft contact lenses of the same curvature fitted on the same eye.

METHODS

The study was prospective and undertaken at a single site, Aston University (Birmingham, UK). Subjects were excluded if they exhibited ocular pathology, dry eye disease, ocular allergy, or corneal irregularity, as were those with a history of recent ocular surgery or previous refractive surgery. Subjects gave written informed consent after an

From ¹Visioncare Research Ltd., Farnham, United Kingdom; ²Aston University, Life and Health Sciences, Ophthalmic Research Group, Birmingham, United Kingdom; and ³Vistakon, Jacksonville, Florida.

Presented at the annual meeting of the British Contact Lens Association Conference, Manchester, United Kingdom, May 2009.

Supported by Johnson & Johnson Vision Care.

Submitted for publication January 6, 2011; revised March 14 and May 23, 2011; accepted June 4, 2011.

Disclosure: L.A. Hall, None; G. Young, None; J.S. Wolffsohn, None; C. Riley, None

Corresponding author: Lee A. Hall, Visioncare Research Ltd., Craven House, West Street, Farnham, Surrey GU9 7EN, UK; l.hall@visioncare.co.uk.

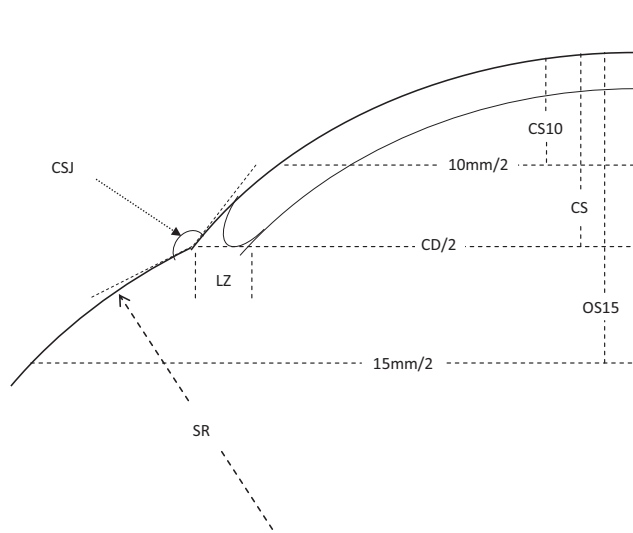


FIGURE 1. OCT ocular topography measurements (see Table 1).

explanation of the nature and possible consequences of the study. The research followed the tenets of the Declaration of Helsinki, and the study protocol was approved by the University's research ethics committee before it was begun.

Fifty subjects' eyes were imaged using a time-domain OCT (Visante; Carl Zeiss Meditec, Dublin, CA) calibrated daily. This instrument allows high-speed,¹⁷ noninvasive, and noncontact¹⁸ in vivo imaging of the anterior segment, capturing full corneal depth and width in one scan,¹⁹ with a resolution of up to 18 μm in the axial and 60 μm in the transverse plane.

OCT images were captured with the eye in the primary-gaze position and also in the four cardinal directions of gaze to give both full sagittal cross-sections of the cornea and cross-sections of the corneoscleral junctions at the superior, inferior, nasal, and temporal positions. Measurements of corneoscleral junction (CSJ) angle, corneal diameter (CD), corneal sagittal height (CS), and scleral radius (SR) were then extracted from the images using the built-in caliper and protractor tools (Fig. 1, Table 1). CD was defined as the distance between the two external scleral sulci. The corneal sagittal height of a chord at 10 mm (CS10) and the ocular sagittal height at 15 mm (OS15) were also taken. Analysis of the OCT images was undertaken using the proprietary curvature correction software, which has been shown to reduce underestimation errors in its measurement of corneal curvature and axial depth.¹⁹

The OCT measurements were tested for intrasession repeatability and reliability by randomly selecting and analyzing 10 different images six times. All readings showed a small measurement error and, therefore, good repeatability: ± 0.14 mm, ± 0.06 mm, $\pm 0.60^\circ$, and ± 7.08 mm for the key ocular variables CD, CS, CSJ angle, and SR, respectively. Intrasession reliability was also good, as evidenced by high intraclass correlation coefficients: 0.89, 0.94, 0.96, and 0.83 (95% confidence interval [CI]) for the same key ocular variables.

Conventional corneal topography data were collected using a corneal topographer (E300; Medmont, Camberwell, Australia), an instrument that has been shown to be both accurate and repeatable.^{20,21} In addition to providing simulated Ks, this also gave corneal height (CS10) and shape factor (SF) data. Subjects' refractions were determined using a validated autorefractor (SRW-5000; Shin-Nippon, Tokyo, Japan).²²

Measurements of horizontal visible iris diameter (HVID) and vertical palpebral aperture (PA) were also extracted from images acquired with a digital slit lamp and image analysis software (SL 990 Digital Vision System; CSO, Firenze, Italy). Limbal zone (LZ) width, the transition zone between the outer edge of the visible iris and the outer corneal sulci, was then determined for each eye as the difference between the horizontal CD and HVID measurements.

From chord diameter and sagittal height measurements, it is possible to calculate the radius of curvature for the equivalent spherical

shape that would align the ocular surface. Equivalent base curves (EBCs) were calculated for each subject using the horizontal CD and CS measurements with the appropriate formula, $([CS^2 + (CD/2)^2]/[2 CS])$. In similar fashion, the EBC was also calculated for each subject's individual topographies for a chord diameter of 15 mm.

Two daily wear soft contact lens types, of power -2.50 D, were evaluated; they were of a conventional hydrogel design (Acuvue 2 [Vistakon]; etafilcon A material, modulus 0.30 MPa) and a silicone hydrogel design (Acuvue Advance [Vistakon]; galyfilcon A material, modulus 0.43 MPa). These lenses were chosen for their similar geometries and identical base curve (8.3 mm) and diameter (14.0 mm). Subjects were randomly assigned to wear one lens design in each eye (i.e., contralaterally). The steepest available base curve (8.30 mm) was selected for dispensing in each case, and lens blister packs were relabeled by a clinical assistant so as to ensure both investigator and subject were masked to lens type.

Lenses were inserted by an investigator and allowed to settle. Comfort and lens fit were then assessed after a minimum of 30 minutes of wear, representative of a lens settled after several hours.^{23,24} Comfort on settling was graded by subjects on a 0 to 10 scale. Four main lens fit variables¹ (the primary end points)—decentration (mm), post-blink movement (mm; PBM), tightness on push-up (%), and overall fit (acceptable/unacceptable)—were assessed by a single experienced investigator to maintain consistency.

Lens centration was measured with respect to the limbus in both the horizontal and the vertical meridians and summated in the post-study analysis to give total decentration. PBM was measured immediately after the blink, with the subject fixating in primary gaze. Measurement was made by observation of the inferior lens edge, and, where necessary, the lower lid was gently displaced to obtain a good view while ensuring minimal displacement of the lens. Lens tightness on push-up was graded on a continuous scale from 0 to 100, where 50 corresponds to the optimum tightness and values above and below 50 signify relatively tighter or looser fits, respectively. Overall fit acceptance was graded as either acceptable or unacceptable, dependent on the investigator's overall assessment of the lens fit.

Statistical Analysis

Pearson's correlation coefficients were used to test for associations between selected clinical, ocular, and lens fit variables. Spearman's correlation coefficients were used to assess the association of these variables with subjective ratings. In view of the risk of type 1 errors with multiple comparisons of association, only those with a $P \leq 0.01$ are presented. Repeated-measure analysis of variance was used to assess the difference in parameters between ocular quadrants.

Multiple regression analysis (forward stepwise method; entry $P = 0.05$, removal $P = 0.10$) was undertaken to determine the predictive

TABLE 1. Abbreviations of Ocular Measurement Variables

Abbreviation	Description
HVID	Horizontal visible iris diameter
PA	Palpebral aperture
K	Simulated keratometry reading
SF	Corneal shape factor ($SF = e^2$)
CD	Corneal diameter
CS	Corneal sagittal height
CS10	Corneal sagittal height of a chord at 10 mm
OS15	Ocular sagittal height of a chord at 15 mm
CSJ	Corneoscleral junction
Δ CSJ	Difference between the two corneoscleral junction angles in a given meridian
LZ	Limbal zone, where $LZ = (CD - HVID)/2$
SR	Scleral radius
EBC	Equivalent (spherical) base curve
n, t, s, i	Nasal, temporal, superior, inferior
h, v	Horizontal, vertical

TABLE 2. Ocular Topography by Videokeratoscopy and Slit Lamp

Ocular Variable	Mean	SD	Median	Range
K, mm				
Flat	7.85	0.26	7.80	7.41-8.73
Steep	7.65	0.25	7.63	7.12-8.51
SF				
Flat	0.43	0.16	0.44	0.00-0.77
Steep	0.21	0.12	0.20	0.00-0.66
CS10, mm (videokeratoscopy)				
Horizontal	1.74	0.08	1.73	1.51-1.89
Vertical	1.81	0.09	1.83	1.57-1.99
PA, mm	10.89	1.36	11.00	6.6-13.43
HVID, mm	11.86	0.56	11.89	9.26-13.22

See Table 1 for abbreviations. $n = 100$ eyes.

values for key fit variables when measured using keratometry alone, keratometry and videokeratoscopy, and, finally, keratometry, videokeratoscopy, and OCT in combination. Ocular topography variables were tested for entry into the model sequentially, based on the significance level of the score statistic. After each entry, variables that were already in the model were tested for possible removal, and variables not included thus far were tested for inclusion. This was repeated until no more variables met entry or removal criteria or until the model remained unchanged.

The analysis was undertaken using statistical software (PASW Statistics V.18; SPSS Inc., Chicago, IL). Missing data were excluded from the analysis and not extrapolated from the collected data.

RESULTS

Biometric Data

Fifty subjects (70% female) were enrolled in and completed the study. The mean age of subjects was 22.8 years (SD ± 5.0 ; range, 18-43). The mean spectacle sphere on autorefraction was -1.97 D (SD ± 2.36 ; range -7.87 to $+2.50$), and the mean spectacle cylinder was -0.64 DC (SD ± 0.50 ; range, 0.00 to -2.12). The ethnicity of subjects was 68% British Asian (individuals of Indian, Pakistani, or Bangladeshi descent) and 18% Caucasian. Three were also identified as Asian/Oriental, three as Afro-Caribbean, and one as mixed race.

A wide range of corneal shapes was measured across the study population (Table 2). Corneoscleral topography results, as assessed by OCT imaging, are summarized in Table 3.

The only measurement derived from both videokeratoscopy and OCT was the measurement of corneal sagittal height for a 10-mm chord (CS10); this showed a significant correlation between the two measurement techniques ($r = +0.69$; $P < 0.0001$; mean difference, 0.03 ± 0.01 mm [95% CI]).

The mean corneoscleral junction (CSJ) angle tended to be sharpest at the nasal CSJ and became progressively flatter at the inferior, temporal, and superior junctions ($F = 102.18$; $P < 0.001$; Table 3). In many cases, CSJ angles were within $\pm 1^\circ$ of 180° , indicating almost tangential extensions of the peripheral cornea to form the sclera. This was evident in 44%, 29%, 12%, and 1% of eyes at the superior, temporal, inferior, and nasal corneoscleral junctions, respectively. The mean differences (95% CI) between opposing corneoscleral junction angles (Δ CSJ), e.g., nasal and temporal, were $4.07^\circ (\pm 0.65)$ and $0.93^\circ (\pm 0.45)$ for the horizontal and vertical meridians, respectively. Scleral radii ranged from 7.5 to 312.5 mm (Table 3). The mean scleral curvature was steepest in the temporal sclera but similar in the nasal, superior, and inferior scleral planes ($F = 10.13$; $P < 0.0001$).

There was a wide variation in LZ width (0.09-2.04 mm); the mean horizontal LZ width was 0.80 mm (SD ± 0.29). The mean EBC for the cornea was 8.64 mm (SD ± 0.33 ; range, 7.27-9.80), and for an ocular chord of 15 mm it was 9.38 mm (SD ± 0.26 ; range, 8.91-10.32).

Lens fit was found to be less variable with the Acuvue 2 lens which tended to show a narrower range of fittings than the Acuvue Advance lens (Table 4). Some extremes of PBM and tightness on push-up were seen with both lens types. However, most fittings fell within what might be regarded as acceptable ranges. For instance, the proportion of fittings exhibiting PBM in the range 0.2 to 0.6 mm was 77%. Overall lens fits were rated as successful for 79% and 88% of the Acuvue Advance and Acuvue 2 lenses, respectively.

A number of lens fit variables were correlated to corneoscleral variables for the silicone hydrogel lens, but the only assessment that correlated with the hydrogel lens was between PBM and PA (Table 5). Modeling of the principal factors of lens fit with corneoscleral measurements showed that central keratometry was a poor predictor of contact lens fit. The addition of videokeratoscopy data did not improve the prediction in this study; however, incorporation of corneoscleral topography from the OCT data strengthened the predictive power of the model. The combined OCT and slit lamp data, for instance, were able to account for 24% of the variance of PBM for the silicone hydrogel lens (Table 6).

DISCUSSION

This study has highlighted a number of interesting findings in relation to the corneoscleral profile. The junction between the cornea and the sclera is often portrayed as a sharp transition given that the radius of the sclera is visibly larger than that of the cornea. However, this study has shown a smooth and, in many cases, tangential transition at the CSJ, with median values

TABLE 3. Ocular Topography Variables by OCT

Ocular Variable	Horizontal				Vertical			
	Mean	SD	Median	Range	Mean	SD	Median	Range
CD, mm	13.39	0.44	13.37	12.10-14.55	13.11	0.57	13.18	11.61-14.96
CS, mm	3.18	0.21	3.17	2.74-3.75	3.07	0.24	3.12	2.45-3.63
CS10, mm	1.76	0.07	1.76	1.53-1.94	1.79	0.07	1.80	1.52-1.94
OS15, mm	3.74	0.16	3.73	3.23-4.10	3.77	0.15	3.78	3.31-4.16
CSJ, deg	173.7 n	3.1	173.7	149.1-179.9	178.3 s	1.7	178.7	167.2-181.1*
	177.6 t	1.6	177.7	172.8-180.0	177.4 i	1.4	177.4	174.0-180.0
SR, mm	45.0 n	41.4	31.4	7.5-312.5	43.1 s	32.2	31.4	-19.7-157.5
	25.3 t	14.8	20.7	12.2-78.8	42.2 i	30.1	31.3	9.4-155.8

See Table 1 for abbreviations. $n = 100$ eyes.

* $>180^\circ$ angle signifies a convex corneoscleral junction profile.

TABLE 4. Lens Fit Results

Lens Fit Variable	Acuvue 2			Acuvue Advance		
	Mean	SD	Range	Mean	SD	Range
Total decentration, mm	0.15	0.13	0.00-0.6	0.22	0.17	0.0-0.8
Horizontal decentration, mm	-0.04	0.14	-0.5-0.2	-0.03	0.12	-0.3-0.2
Vertical decentration, mm	0.03	0.13	-0.4-0.3	0.12	0.22	-0.6-0.8
Post-blink movement, mm	0.33	0.17	0.00-0.80	0.25	0.14	0.00-0.60
Lens tightness, push-up test, %	40.7	9.5	20-60	41.9	9.9	20-65

n = 50.

of 179° and 178° at the superior and temporal junctions, respectively. This apparent contradiction arises because of there being a gradual transition in topography between the cornea and the sclera, with the sclera adopting its true radius some millimeters from the limbus.

Meier¹² also noted a tangential corneoscleral profile in a majority of eyes when visually examining the superior profile in a large proportion of subjects. It was suggested that this assessment of superior CSJ might be used to predict soft contact lens fit; however, this seems optimistic given the variation in CSJ between different meridians noted in this study. The fact that CSJ angles were sharper at the nasal junction is consistent with the findings of Marriott,¹¹ who noted different scleral topography nasally compared with the other three quadrants and ascribed this to the insertion of the medial rectus muscle being closest to the cornea.

The mean CD as assessed using OCT was greater than the HVID measured using traditional image capture. There was a wide range of CDs among the sample, and the horizontal meridian was wider than the vertical, as expected ($P < 0.0004$; $t = 3.70$). The mean HVID was similar to that noted in previous studies,²⁵⁻²⁷ but the mean horizontal CD of 13.39 mm (SD ± 0.44) was slightly greater than the measurements of Martin and Holden,²⁵ who found a mean corneal diameter of 12.9 mm (SD ± 0.6) using a photographic method.

The use of OCT allowed for a characterization of the limbal transition zone (LZ) based on the difference between HVID and the horizontal CD. There was a wide variation in LZ width, which emphasized the poor reliability of HVID measurements in characterizing corneal size.²⁸ This was primarily attributed to the difficulty in defining visible iris diameter, which itself depends on the rate of loss of transparency of the peripheral cornea.

As hypothesized, lens fit tended to be more variable with the stiffer silicone hydrogel lens, which, despite having a similar profile, showed fewer acceptable fittings than the hydrogel lens. A number of corneoscleral measures were correlated to lens fit variables for the silicone hydrogel lens, whereas, with the lower modulus lens, the only correlation was between PBM

and PA. Modeling of the principal components of lens fit confirmed that central keratometry was a poor predictor of contact lens fit. The addition of the videokeratoscopy data did not improve the prediction; however, the incorporation of corneoscleral topography data allowed better prediction of lens fit, especially for the silicone hydrogel contact lens. It seems probable that the higher elastic modulus of the silicone material prevented it from wrapping as closely to the corneoscleral shape as a conventional hydrogel contact lens, resulting in less friction and more interaction between the lid and lens profile.

With respect to decentration of the hydrogel lens, the predictive ability of keratometry along the flat meridian was outperformed by the OCT measurement of nasal scleral curvature. The greater influence of the horizontal meridian is probably due to the asymmetry in CSJ angles between the nasal and temporal quadrants. Interestingly, decentration with the stiffer silicone hydrogel lens was less well predicted by corneal shape, but the predictive ability of the scleral radius was greater.

Variance in PA consistently allowed for the prediction of 13% to 18% of PBM, with the difference in CSJ angles between the nasal and temporal quadrants (Δ CSJh) also explaining an additional 7% of variance for the silicone hydrogel lens. The influence of PA can be explained by the effect of the area of friction between the eyelids and the lens surface and, hence, the speed of post-blink lens recovery. In addition, the eyelid has to travel further to cover a wider PA, resulting in more interaction with the lens surface, increasing the movement during blink and, hence, PBM.

Differences in nasal and temporal CSJ angles relate to asymmetry of the horizontal sclera. With Acuvue Advance, larger differences in the horizontal CSJ angles (Δ CSJh) were associated with increased lens tightness on push-up. As differences in CSJ angle increase, it is likely that the lens is forced to undergo greater stretching and flexing in the periphery to align with the corneoscleral topography, leading to greater inner elastic forces and increased tightness. The fact that corneal sagittal height in the vertical meridian

TABLE 5. Significant Lens Fit Correlations with Corneoscleral Shape Parameters

Lens Fit Variable	Lens Type	Ocular Variable	Correlation Coefficient (<i>r</i>)	<i>P</i>
Comfort	AA	CS10h (by Videokeratoscopy)	-0.39	0.0062
Lens tightness	AA	Δ CSJh	+0.40	0.0041
Post-blink movement	A2	PA	+0.39	0.0086
Post-blink movement	AA	PA	+0.44	0.002
Total decentration	AA	SRt	+0.37	0.0091
Horizontal centration	AA	CS10h (by OCT)	-0.38	0.0065
Horizontal centration	AA	CS10v (by OCT)	-0.39	0.0056
Vertical centration	AA	SRt	+0.47	0.0005

n = 50. AA, Acuvue Advance; A2 = Acuvue 2 lenses.

TABLE 6. Stepwise Multiple Regression Analysis

Lens Type	Outcome Variable	Keratometry			Keratometry and Videokeratometry			Keratometry, Videokeratometry, and OCT			
		Predictor Variables	Adjusted R ²	P	Predictor Variables	Adjusted R ²	P	Predictor Variables	Adjusted R ²	P	
Acuvue 2	Total decentration	Constant Kf	0.024 0.043	0.06	0.024 0.043	0.06	0.043	Constant SRn	0.020 0.024	0.08	0.024
	Movement	Constant PA	0.13 0.0020	0.18	Constant PA	0.13 0.0020	0.002	Constant PA	0.13 0.0020	0.18	0.002
	Tightness	No significant predictor variables			No significant predictor variables			Constant CS10v	0.0007 0.022	0.09	0.022
Acuvue Advance	Total decentration	No significant predictor variables			No significant predictor variables			Constant SRt	0.0038 0.0091	0.12	0.009
	Movement	Constant PA	0.32 0.0086	0.13	Constant PA	0.32 0.0086	0.009	Constant PA	0.63 0.0060	0.24	0.002
	Tightness	No significant predictor variables			No significant predictor variables			Constant ΔCSAh	0.014 0.0001	0.14	0.004

(as opposed to ΔCSJh) predicted tightness with the Acuvue 2 lens may be attributable to the lower modulus of etafilcon A, resulting in more forgiving alignment of the lens to the corneoscleral topography.

Although corneoscleral topography accounts for more of the variance in soft lens fit than corneal topography alone, approximately three-quarters of the variance remains unexplained. This may be partly explained by a number of limitations in the present study design. The model compared linear association between the topography and lens fit variables, whereas the interactions may be more complex. The ratings of contact lens fit were observational, and the variability, even in an experienced observer, will weaken the associations with corneoscleral topography. The contact lens designs used in this study exhibited a relatively narrow range of fitting behaviors, and it is possible that more varied lens designs would have revealed stronger associations. It is also possible that a larger sample may have revealed a wider range of ocular topographies which, in turn, may have revealed stronger relationships. A larger scale study providing ocular topography data on subjects with a wider range of refractions, ages, and ethnicities will form the subject of a future paper.

Kikkawa²⁹ described a model in which a soft contact lens could be considered as a series of concentric elastic rubber bands, progressively stretching and flexing to accommodate changes in peripheral ocular curvature. It is likely that the enforced change in lens radius for a lens to align to the scleral surface may result in raised squeeze pressure at the lens periphery, in turn explaining why some lens fits appear excessively 'tight' or 'loose'. The use of OCT enabled the measurement of CD and CS, but also ocular sagittal height at a chord roughly equivalent to soft contact lens diameter (15 mm). The EBC for the cornea was close to that of a typical soft lens but was appreciably flatter for the wider 15-mm chord (8.6 vs. 9.4 mm). This suggests that most flexure of the type described by Kikkawa²⁹ takes place in the lens periphery.

More work is needed to understand the ocular factors governing lens fit. Given the wide range of variables, useful information might be gained from computer modeling that would allow the control of all but one or two variables. An alternative approach for future clinical work would be to examine the corneal topography of patients with known fitting problems, specifically 'tight' or 'loose' lens fits.

In conclusion, the measurement of corneal topography using an OCT technique allows for a more complete characterization of the cornea and peripheral corneoscleral profile than either conventional keratometry or videokeratometry. The extra peripheral corneoscleral data gained from OCT characterization of ocular surface architecture provide valuable insight into soft contact lens fit dynamics.

Acknowledgments

The authors thank their co-investigators Sarah Humphries and Amy Sheppard.

References

1. Young G. Evaluation of soft contact lens fitting characteristics. *Optom Vis Sci.* 1996;73:247-254.
2. Young G, Coleman S. Poorly fitting soft lenses affect ocular integrity. *Cont Lens Assoc Ophthalmol.* 2001;27:68-74.
3. Knop E, Brewitt H. Conjunctival cytology in asymptomatic wearers of soft contact lenses. *Graefes Arch Clin Exp Ophthalmol.* 1992; 230:340-347.
4. Young G. Why one million contact lens wearers dropped out. *Cont Lens Anterior Eye.* 2004;27:83-85.

5. Snyder AC. Cosmetic extended-wear lenses: considering sagittal differences between the lens and eye. *Int Contact Lens Clinic*. 1984;11:613-624.
6. Garner L. Sagittal height of the anterior eye and contact lens fitting. *Opt Phys Opt*. 1982;59:301-305.
7. Young G, Schnider, Hunt C, Efron S. Corneal topography and soft contact lens fit. *Optom Vis Sci*. 2010;87:358-366.
8. Gundal R, Cohen H, DiVergillio D. Peripheral keratometry and soft contact lens fitting. *Int Eyecare*. 1986;2:611-613.
9. Hansen D. Evaluating the eye with corneal topography. *Cont Lens Spectrum August*. 2003;27-32.
10. Caroline PJ, André MP, Norman CW. Corneal topography and computerised lens-fitting modules. *Int Contact Lens Clinic*. 1994;21:185-195.
11. Marriott PJ. An analysis of the global contours and haptic contact lens fitting. *Br J Physiol Opt*. 1966;23:1-40.
12. Meier D. Das corneo-skleral-profil-ein kriterium individueller kontaktlinsen-anpassung. *Die Kontaktlinse*. 1992;26:4-11.
13. Bibby M. A model for lens flexure—validation and predictions. *Int Contact Lens Clinic*. 1979;7:124-138.
14. Kaluzny J, Wojtkowski M, Kowalczyk A. Imaging of the anterior segment of the eye by spectral optical tomography. *Opt Appl*. 2002;32:581-589.
15. Kaluzny BJ, Kaluzny JJ, Szkulmowska A, et al. Spectral optical coherence tomography: a new imaging technique in contact lens practice. *Ophthalm Physiol Opt*. 2006;26:127-132.
16. Shen M, Wang M, Wang J, Yuan Y, Chen F. Entire contact lens imaged in vivo and in vitro with spectral domain optical coherence tomography. *Eye Contact Lens*. 2010;36:73-76.
17. Sakata L, Wong Y, Wong H, et al. Comparison of Visante and slit-lamp anterior segment optical coherence tomography in imaging the anterior chamber angle. *Eye*. 2010;24:578-587.
18. Leung C, Cheung C, Li H, et al. Dynamic analysis of dark-light changes of the anterior chamber angle with anterior segment OCT. *Invest Ophthalmol Vis Sci*. 2007;48:4116-4122.
19. Dunne M, Davies L, Wolffsohn J. Accuracy of cornea and lens biometry using anterior segment optical coherence tomography. *J Biomed Opt*. 2007;12:064023.
20. Tang W, Collins MJ, Carney L, Davis B. The accuracy and precision performance of four videokeratoscopes in measuring test surfaces. *Optom Vis Sci*. 2000;77:483-491.
21. Cho P, Lam AKC, Mountford J, Ng L. The performance of four different corneal topographers on normal human corneas and its impact on orthokeratology lens fitting. *Optom Vis Sci*. 2002;79:175-183.
22. Mallen E, Wolffsohn J, Gilmartin B, Tsujimura S. Clinical evaluation of the Shin-Nippon SRW-5000 autorefractor in adults. *Ophthalm Physiol Opt*. 2001;21:101-107.
23. Brennan N, Lindsay R, McCraw K, Young L, Bruce A, Golding T. Soft lens movement: temporal characteristics. *Optom Vis Sci*. 1994;71:359-363.
24. Golding T, Bruce A, Gaterell L, Little S, MacNamara. Soft lens movement: effect of blink rate on lens settling. *Acta Ophthalm Scand*. 1995;73:506-511.
25. Martin DK, Holden BA. A new method for measuring the diameter of the in vivo human cornea. *Am J Optom Physiol Opt*. 1982;59:436-441.
26. Matsuda L, Woldorff, Kame R, Hayashida J. Clinical comparison of corneal diameter and curvature in Asian eyes with those of Caucasian eyes. *Optom Vis Sci*. 1992;69:51-54.
27. Theodorff C, Lowther G. Quantitative effect of optic zone diameter changes on rigid gas permeable lens movement and centration. *Int Cont Lens Clinic*. 1990;17:92-95.
28. Kwok LS. Measurement of corneal diameter (letter). *Br J Ophthalmol*. 1990;74:63-64.
29. Kikkawa Y. Kinetics of soft contact lens fitting. *Contacto*. 1979;23:10-17.